

1 **Pre-Cordilleran mantle metasomatism preserved in alkali basalts of Isla**
2 **Isabel, México**

3
4 Leonie Sieger, Bradley J. Peters*, Andrea Giuliani, Maria Schönbächler

5
6 Institute of Geochemistry and Petrology, ETH Zürich, CH-8092 Zürich, Switzerland

7 *Corresponding author: bradley.peters@erdw.ethz.ch

8
9 Submitted to *Geology*

10 This is a non-peer reviewed preprint uploaded to EarthArXiv

11
12 Character count (including spaces): 18,579

13 Tables: 1

14 Figures: 3

15
16 Supplementary text and figures accompany this article.

17 **Abstract**

18 The presence of HIMU (high- $^{238}\text{U}/^{204}\text{Pb}$) signatures in ocean island basalts has long been used to argue
19 that ancient oceanic crust has been tectonically recycled into the mantle sources of plume-derived
20 volcanic hotspots such as St. Helena or Mangaia. However, alternative hypotheses regarding the origins
21 of HIMU signatures have also been put forward. This paper addresses the origins of HIMU-like Pb
22 isotopic signatures in Isla Isabel, a small ($\sim 1 \text{ km}^2$) intraplate volcanic island located off the western coast
23 of México, southeast of the southern tip of Baja California. The Nd-Hf isotopic signatures of Isla Isabel
24 are nearly identical to St. Helena and Mangaia, however since there is no mantle plume underlying Isla
25 Isabel it is unlikely that these signatures derive from recycled oceanic crust. We argue that Isla Isabel
26 lavas were instead produced by mixing of depleted mantle-like material and continental lithospheric
27 mantle that was metasomatized $\geq 600 \text{ Ma}$ ago, an age that overlaps with the regional breakup of Rodinia.
28 Such preservation of ancient tectonic events is remarkable, since the exposed geological record in
29 continental México preserves a very limited record of geological events older than the Mexican
30 Cordillera ($< 165 \text{ Ma}$). Isla Isabel therefore illustrates that the origins of HIMU-type intraplate lavas are
31 not limited to ancient recycled oceanic crust. Rather, they can also preserve information about the
32 evolution of the upper mantle through large-scale tectonic cycles, even when these events have been
33 otherwise erased from the surficial rock record.

34 Introduction

35 Isla Isabel is an intraplate volcanic island overlying the western México continental shelf (**Fig. 1**) that
36 hosts HIMU-like isotopic signatures with undetermined provenance (Housh et al., 2010). The geological
37 history of the region surrounding Isla Isabel is complex. Subduction of the Farallon Plate generated
38 volcanism in northwestern México until 12 Ma ago, when seafloor spreading along the Pacific-
39 Guadalupe Ridge ended and subduction in this region ceased (Lonsdale, 1991). Subsequently, the
40 volcanic arc migrated southward to the presently active Trans-Mexican Volcanic Belt (TMVB; e.g.,
41 Ferrari et al., 2012) and northwestern México transitioned to an extensional tectonic regime, marked
42 most notably by the opening of the Gulf of California (Lonsdale, 1991). Isla Isabel lies on the extended
43 strike of the TMVB onto the continental shelf, toward the Gulf of California, and is located ca. 100 km
44 north of the northernmost extent of the subduction zone. Thus, it is considered unlikely the ca. 5 Ma
45 volcanic history of Isla Isabel is related to regional subduction; rather, it is thought to be related to local
46 extension from the prior regional tectonic reorganization (Housh et al., 2010).

47 Intraplate basalts with broadly similar geochemical compositions to Isla Isabel occur in northwestern
48 mainland México (Aranda-Gómez et al., 2007) and within the TMVB (Díaz-Bravo et al., 2014). The
49 radiogenic Pb isotopic and olivine major element compositions of these rocks have been attributed to
50 metasomatism of the mantle wedge underlying the active and paleo-volcanic arcs and to crustal
51 assimilation. Isla Isabel presents a complementary perspective on the sub-Mexican mantle in that its
52 geochemistry is largely unaffected by either subduction or crustal assimilation processes (Housh et al.,
53 2010). Alkali basalts are also found on islands several hundred km southwest of Isla Isabel that overlie
54 oceanic, rather than continental lithosphere. Two of these islands, Socorro and Guadalupe, are generated
55 by mantle plumes imaged by seismic tomography that extend through 30-40% of the total mantle depth
56 (e.g., Koppers et al., 2021); by contrast, no mantle plume is known to underlie Isla Isabel.

57 A previous study of Isla Isabel basalts identified their distinct geochemical and isotopic compositions
58 compared to the arc-related volcanic rocks of the TMVB (Housh et al., 2010). Notably, like intraplate-
59 type basalts from the TVMB (Díaz-Bravo et al., 2014), their Pb isotope signatures trend toward those
60 of HIMU (high $\mu = {}^{238}\text{U}/{}^{204}\text{Pb}$) ocean island basalts (OIB; Housh et al., 2010). HIMU is one of several
61 theoretical mantle components, which among OIB is most commonly associated with recycling of
62 ancient (>2 Ga old) subducted oceanic crust (e.g., Chauvel et al., 1995; Stracke et al., 2005; Nebel et al.,
63 2013). The HIMU component is classically found in OIB from Mangaia and St. Helena (Zindler and
64 Hart, 1986; Stracke et al., 2005), although the Pb isotopic signature of Isla Isabel lavas is not as
65 radiogenic as in these localities (Housh et al., 2010). HIMU-like isotope compositions have also been
66 identified in continental intraplate rocks unrelated to recycled subducted crust, and ancient mantle
67 metasomatism has been proposed for an alternative mechanism to generate highly radiogenic Pb
68 signatures (Ballentine et al., 1997; Rooney et al., 2014; cf., Díaz-Bravo et al., 2014). This paper uses
69 combined Sr-Nd-Hf-Pb isotopic and trace element compositions to clarify the origins of the HIMU-like

70 isotope signatures of Isla Isabel lavas and to determine whether intraplate magmas can provide
71 constraints on the geochemical evolution of the mantle during tectonic reorganization processes.

72

73 **Methods and Results**

74 Nine Isla Isabel samples, originally studied by Housh et al. (2010) were analyzed for their ^{87}Sr - ^{143}Nd -
75 ^{176}Hf - $^{206,207,208}\text{Pb}$ isotopic compositions. Full details of analytical methods are given in the
76 Supplementary Information. Isla Isabel samples have homogeneous Sr-Nd-Hf-Pb isotopic compositions
77 (**Table 1**). The combined Sr-Nd-Pb isotopic signatures of Isla Isabel lavas plot at the edge of the TMVB
78 arrays or extend these arrays and overlap the compositional fields of global non-hotspot intraplate basalts
79 (**Fig. 2**). Their Sr and Nd isotopic compositions are intermediate between depleted mid-ocean ridge
80 basalt (MORB) mantle (DMM, e.g., East Pacific Rise MORB) and highly enriched isotopic
81 compositions (EM) and are dissimilar to HIMU-type OIB (**Fig. 2a**). The average $^{206}\text{Pb}/^{204}\text{Pb}$ ratio of Isla
82 Isabel basalts is 19.330 ± 0.027 (2 s.d.), significantly less radiogenic than classical HIMU-type OIB but
83 more radiogenic than DMM or TMVB lavas (**Fig. 2b**). The $^{208}\text{Pb}^*/^{206}\text{Pb}^*$ compositions of Isla Isabel
84 lavas also differ from both DMM and classical HIMU lavas (**Fig. 2c**). By contrast, their Nd and Hf
85 isotopic signatures fall below the mantle array and are almost identical to the Nd-Hf isotopic signatures
86 of classical HIMU hotspots (**Fig. 2d**), making them clearly distinct from nearly all other global non-
87 hotspot intraplate lavas.

88

89 **Discussion**

90 **Comparison of HIMU-like signatures in Isla Isabel**

91 The Nd-Hf isotopic compositions of Isla Isabel lavas (**Fig. 2d**) imply that they may share a common
92 history with classical HIMU OIB. The location of the samples below the mantle array indicates their
93 sources tap a mantle component that has experienced a past enrichment event that produced lower
94 Sm/Nd and Lu/Hf ratios compared to the sources of lavas that lie on the mantle array. The less radiogenic
95 $^{176}\text{Hf}/^{177}\text{Hf}$ for a given $^{143}\text{Nd}/^{144}\text{Nd}$ ratio exhibited by HIMU lavas relative to other OIB has been
96 previously attributed to fractionation events that were more extreme with respect to Lu-Hf than Sm-Nd,
97 resulting in long-term decoupling of the two isotope ratios (cf., Nebel et al., 2013). The amount of
98 decoupling depends on both the timing and the degree of fractionation between the corresponding parent
99 and daughter elements (Chauvel et al., 2008). Classical HIMU are generally associated with geologically
100 old (>2 Ga) sources, because this allows simultaneous generation of very radiogenic Pb and relatively
101 unradiogenic Sr, Nd, and Hf isotopic signatures. However, an alternative hypothesis holds that HIMU-
102 like isotopic signatures can be generated by mantle metasomatism in little as 200 Ma (e.g., McCoy-West
103 et al., 2016).

104 Isla Isabel lavas possess less radiogenic Pb isotopic signatures (**Fig. 2c**) compared to HIMU OIB
105 localities. Additionally, their combined $^{208}\text{Pb}^*/^{206}\text{Pb}^*$ compositions, which record the long-term Th/U
106 ratio of its mantle source, are incompatible with mixing between DMM and an OIB HIMU component
107 (**Figs. 1c, S1**). Instead, the Pb isotopic compositions of Isla Isabel lavas lie along an array of global non-
108 hotspot intraplate lavas with $^{207}\text{Pb}/^{204}\text{Pb}$ - $^{206}\text{Pb}/^{204}\text{Pb}$ compositions that link depleted isotopic signatures
109 (e.g., MORB) with an ancient enriched Pb isotopic signature (**Fig. S2**). For example, the Isla Isabel Pb
110 isotopic signature can be modeled as a mixture of EPR-like depleted material and an enriched Pb isotopic
111 component that was introduced 600 Ma ago and raised both the Pb isotopic ratios and the U/Pb ratio of
112 the Isla Isabel mantle source (**Fig. S2**). Introduction of this component at ages like those expected for
113 HIMU OIB would instead require that the Isla Isabel source has a low U/Pb ratio, less than that of the
114 depleted mantle. Further, Isla Isabel lavas lack the strongly positive Nb anomalies associated with
115 recycled crust (e.g., Cordier et al., 2021); instead, they have Ce/Pb and $\text{Nb}_\text{N}/\text{Nb}^*$ ratios that resemble
116 DMM (e.g., Arevalo & McDonough, 2010; **Fig. S3**). Finally, Isla Isabel olivine have high CaO and low
117 NiO compositions (Housh et al., 2010; **Fig. S4**) that require their derivation from peridotite rather than
118 mantle pyroxenite associated with subducted oceanic crust (e.g., Herzberg et al., 2014). A similar
119 observation was previously reported for intraplate-type basalts from the TMVB (Díaz-Bravo et al.,
120 2014), implying that pyroxenite signatures are generally absent from the regional mantle.

121 Modern HIMU-type OIB associated with geochemical signatures of recycled oceanic crust are spatially
122 associated with deep mantle plumes (Jackson et al., 2018). By contrast, there is no known mantle plume
123 beneath Isla Isabel or in the region of northwestern México (Smith, 1999; Mora-Klepeis, 2021; Koppers
124 et al., 2021) that would be capable of delivering deeply recycled oceanic crust to the melting region of
125 Isla Isabel. Recycling of subducted crust at shallower mantle depths is also unlikely due to the higher
126 density of subducted crust, which transforms to eclogite in subduction zones, compared to upper mantle
127 peridotites (Brandenburg et al., 2008). Alternatively, ancient mantle plumes and fluids released during
128 subduction can metasomatize the upper mantle and change local isotopic evolution pathways (e.g.,
129 Homrighausen et al., 2018). For example, a CO_2 -rich metasomatic origin for the classical HIMU island
130 Mangaia was also evaluated (Weiss et al., 2016), and a single analysis of CO_2 in a basaltic glass from
131 Isla Isabel (Housh et al., 2010) yielded a CO_2 abundance similar to those of melt inclusions from
132 Mangaia (Cabral et al., 2014). Therefore, an ancient metasomatic origin is most likely for Isla Isabel.
133 This interpretation has also been invoked for other non-hotspot intraplate basalts, for example HIMU-
134 like intraplate lavas from Africa are argued to be related to melting of amphibole-rich metasomes that
135 were generated 700 Ma ago (Rooney et al., 2014).

136

137 **A pre-Cordilleran metasomatic origin of Isla Isabel HIMU signatures**

138 To determine the origin of Isla Isabel's distinct isotope composition, a solid-state mixing model between
139 convecting, depleted upper mantle (DMM; compositions from Salters & Stracke, 2004 and Workman

140 & Hart, 2005) and metasomatized continental lithospheric mantle (CLM; compositions based on Wittig
141 et al., 2010, see Supplementary Information) is applied to the collected data. The calculated $\Delta\epsilon^{176}\text{Hf}$ and
142 $^{207}\text{Pb}/^{206}\text{Pb}$ compositions of the metasomatized component depend in part on the time this metasomatism
143 occurred, with earlier metasomatism producing lower $\Delta\epsilon^{176}\text{Hf}$ and $^{207}\text{Pb}/^{206}\text{Pb}$ if the effect of
144 metasomatism on parent-daughter ratios is held constant. One constraint on this age is provided by the
145 Hf model ages of the Isla Isabel samples ($\tau_{176} = 616 \pm 35$ Ma, 2 s.d.). Although this likely provides only
146 a minimum age for the time of metasomatism (Supplementary Information), it is the only contextualized
147 age information available for the mantle source of Isla Isabel.

148 This model produces a mixing curve between modern DMM and metasomatized CLM that passes
149 through both the Isla Isabel data and, at higher proportions of metasomatized mantle, also passes through
150 literature data for Mangaia (**Fig. 3**). A relatively high proportion of a fusible, metasomatized CLM
151 component beneath Isla Isabel may have promoted mantle melting when the mantle lithosphere was
152 reactivated by recent tectonic reorganization (cf., Hoernle et al., 2011), thus providing an explanation
153 for localized volcanism. By contrast, a model representing 3 Ga old recycled oceanic crust (cf., Nebel
154 et al., 2013) can also reproduce the isotopic composition of Mangaia and St. Helena rocks (cf., Nebel et
155 al. (2013), but not Isla Isabel signatures. In both cases, the model uses a global average DMM value as
156 the depleted mixing component, although MORB from a geographically close location to Isla Isabel,
157 e.g., the northern East Pacific Rise (NEPR), have slightly negative $\Delta\epsilon^{176}\text{Hf}$ values. These compositions
158 can be explained analogously to those of Isla Isabel, however in this case the metasomatic CLM
159 component must be either older or possess more enriched Lu/Hf-Sm/Nd ratios (cf., **Fig. 3**, “alternative”
160 model). In this context, the $\Delta\epsilon^{176}\text{Hf}$ compositions of Isla Isabel and NEPR samples may reflect pervasive
161 dispersion of variably metasomatized Mexican CLM throughout the continental and oceanic lithosphere
162 along the Mexican margin.

163 The origin of the Isla Isabel mantle metasomatic component cannot be related to the modern subduction
164 zone, since the Hf isotopic compositions of the Isla Isabel rocks likely require that their mantle source
165 differentiated from the depleted mantle at least 600 Ma ago, whereas the Farallon Plate is likely less
166 than 165 Ma old (e.g., Engebretson et al., 1985). By contrast, surficial volcanic rocks in México provide
167 only a limited record of tectonic events prior to the generation of the Mexican Cordillera. For example,
168 collisional-extensional regimes related to the assembly and breakup of the Precambrian supercontinent
169 Rodinia are preserved only by the Oaxaquia microplate of southern México, ca. 1200 km SE of Isla
170 Isabel (e.g., Keppie and Ortega-Gutiérrez, 2010). The last of these preserved extensional events occurred
171 between 750 and 545 Ma ago, an age that overlaps the Hf model ages of the studied Isla Isabel samples
172 and thus provides a potential explanation for their negative $\Delta\epsilon^{176}\text{Hf}$ compositions (**Fig. 3**). The
173 lithospheric mantle beneath Isla Isabel may therefore preserve a geochemical memory of events related
174 to ancient supercontinent cycles that have been largely overprinted on the Mexican mainland. Dispersed
175 metasomatized CLM in other localities may similarly preserve geochemical information about ancient

176 tectonic events but this is only exceptionally unlocked by non-hotspot intraplate volcanoes such as Isla
177 Isabel.

178

179 **Conclusion**

180 Combined Sr-Nd-Hf-Pb isotopic compositions for the intraplate volcanic island Isla Isabel reflect a
181 HIMU-type mantle source that was likely generated by ancient metasomatic event affecting Mexican
182 CLM. Dispersal of this component to a relatively high degree under Isla Isabel, and possibly to a lesser
183 extent throughout the regional oceanic mantle, generated the HIMU-like isotopic characteristics Isla
184 Isabel basalts. Hafnium isotopic compositions constrain the age of the metasomatic event to be older
185 than Mesozoic-to-recent subduction of the Farallon Plate that produced the Mexican Cordillera. This
186 demonstrates that the utility of HIMU-type intraplate lavas is not limited to understanding ancient
187 subduction of oceanic crust; rather, they can provide critical access to other ancient tectonic processes
188 for which few remnants remain in the accessible geological record.

189

190 **Acknowledgements**

191 Many thanks go to Marc Halfar for his help during laboratory preparations. Samples for this project
192 were loaned by the Smithsonian Natural History Museum. Financial support for this research was
193 provided by the Swiss National Science Foundation (PZ00P2_180005 to BJP and PZ00P2_180126/1 to
194 AG) and ETH Zürich operational funding.

195 **Table and Figures**196 **Table 1.** Sr, Nd, Hf and Pb isotope data of Isla Isabel samples.

Sample	$^{87}\text{Sr}/^{86}\text{Sr}$	2SD	n (n_d) ^a	ϵNd ^b	2SD	n (n_d) ^a	ϵHf ^b	2SD	n (n_d) ^a	$^{206}\text{Pb}/^{204}\text{Pb}$	2SD	$^{207}\text{Pb}/^{204}\text{Pb}$	2SD	$^{208}\text{Pb}/^{204}\text{Pb}$	2SD	n (n_d) ^a
NAY-2	0.703267	0.000009	1 (1)	5.14	0.05	4 (1)	4.66	0.54	2 (1)	19.3049	0.0012	15.6430	0.0013	38.9373	0.0042	7 (1)
NAY-3	0.703285	0.000009	3 (2)	5.03	0.05	4 (2)	5.55	0.09	7 (2)	19.3559	0.0010	15.6488	0.0009	39.0148	0.0030	12 (2)
NAY-4	0.703260	0.000009	1 (1)	4.97	0.07	2 (1)	5.38	0.27	2 (1)	19.3269	0.0012	15.6465	0.0015	38.9600	0.0054	7 (1)
NAY-13	0.703251	0.000009	1 (1)	4.92	0.07	2 (1)	4.96	0.25	2 (1)	19.3317	0.0006	15.6507	0.0006	38.9762	0.0022	7 (1)
NAY-14	0.703245	0.000009	1 (1)	4.92	0.07	2 (1)	5.59	0.27	2 (1)	19.3364	0.0026	15.6566	0.0031	38.9952	0.0101	8 (1)
NAY-15	0.703253	0.000009	1 (1)	5.00	0.08	2 (1)	5.49	0.24	2 (1)	19.3324	0.0011	15.6483	0.0012	38.9688	0.0041	6 (1)
NAY-31	0.703256	0.000009	1 (1)	4.96	0.07	2 (1)	5.62	0.17	2 (1)	19.3275	0.0009	15.6450	0.0009	38.9567	0.0029	7 (1)
NAY-32	0.703224	0.000009	1 (1)	5.13	0.07	2 (1)	5.75	0.17	2 (1)	19.3234	0.0009	15.6392	0.0011	38.9282	0.0036	7 (1)
NAY-35	0.703250	0.000009	1 (1)	4.95	0.07	2 (1)	5.46	0.17	2 (1)	19.3287	0.0010	15.6468	0.0010	38.9637	0.0034	11 (1)
BHVO-2 ^c	0.703470	0.000009	1 (1)	6.99	0.04	8 (1)	10.81	0.10	6 (1)	18.5980	0.0003	15.5368	0.0004	38.1930	0.0010	7 (1)

197

198 *Notes:*

198

199 ^a n refers to number of individual analyses, n_d refers to number of separate digestions of a given sample.

199

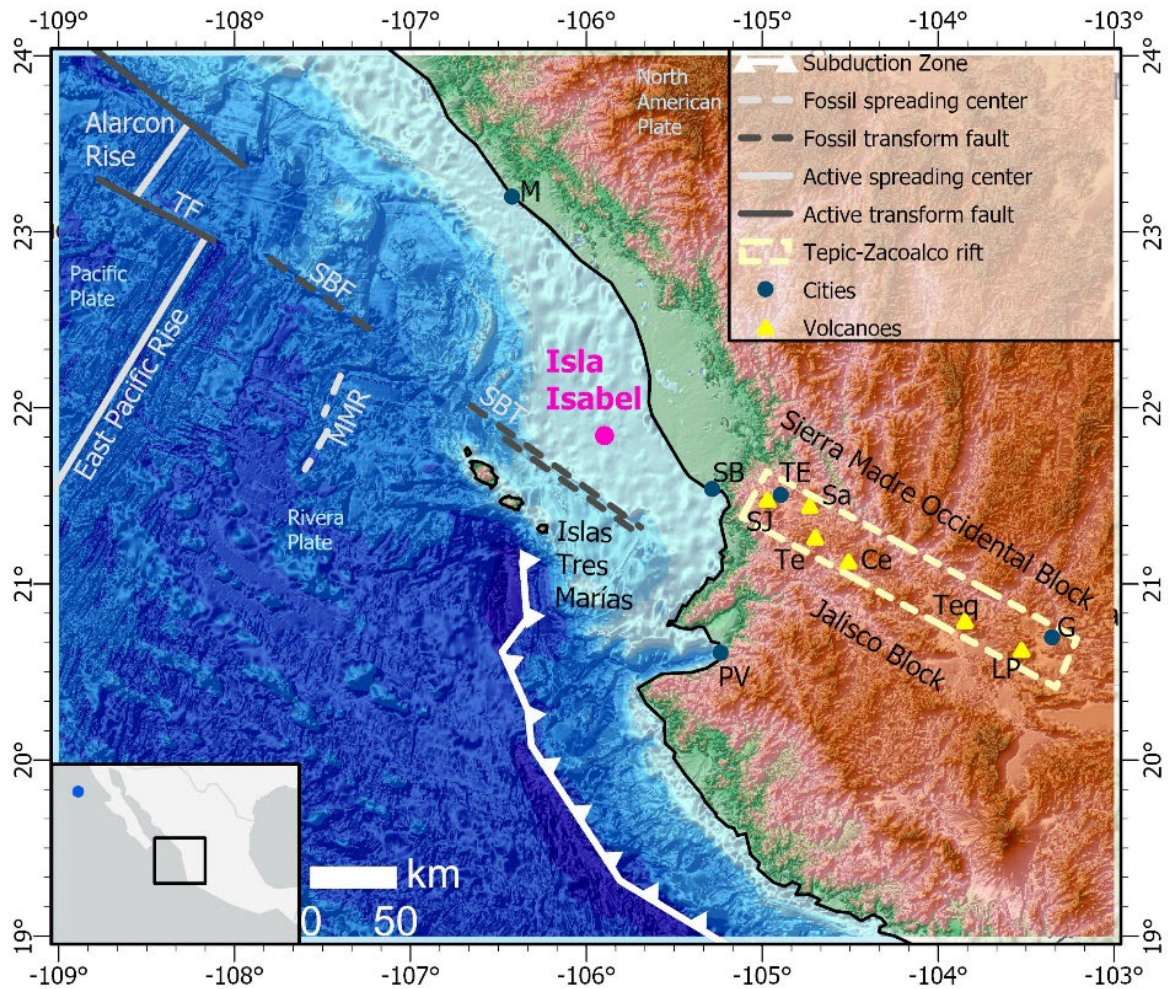
200 ^b Epsilon notation normalised to CHUR values $^{176}\text{Hf}/^{177}\text{Hf} = 0.282785$ and $^{143}\text{Nd}/^{144}\text{Nd} = 0.512630$ (Bouvier et al., 2008).

200

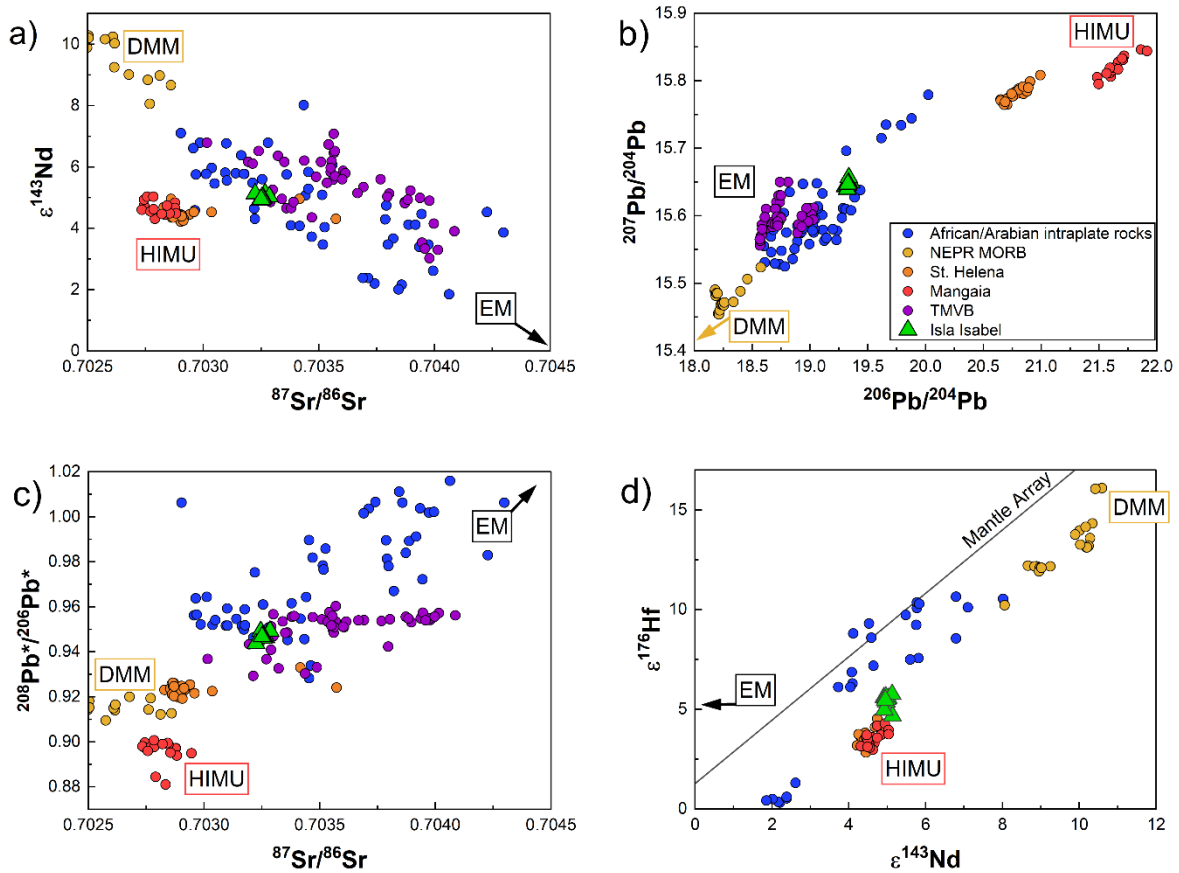
201 ^c Measured BHVO-2 values are within reference values reported by Weis et al. (2005): $^{176}\text{Hf}/^{177}\text{Hf} = 0.283096 \pm 20$, $^{143}\text{Nd}/^{144}\text{Nd} = 0.512983 \pm 10$, $^{206}\text{Pb}/^{204}\text{Pb} =$
202 18.6173 ± 465 , $^{207}\text{Pb}/^{204}\text{Pb} = 15.5355 \pm 54$, $^{208}\text{Pb}/^{204}\text{Pb} = 38.2108 \pm 384$.

201

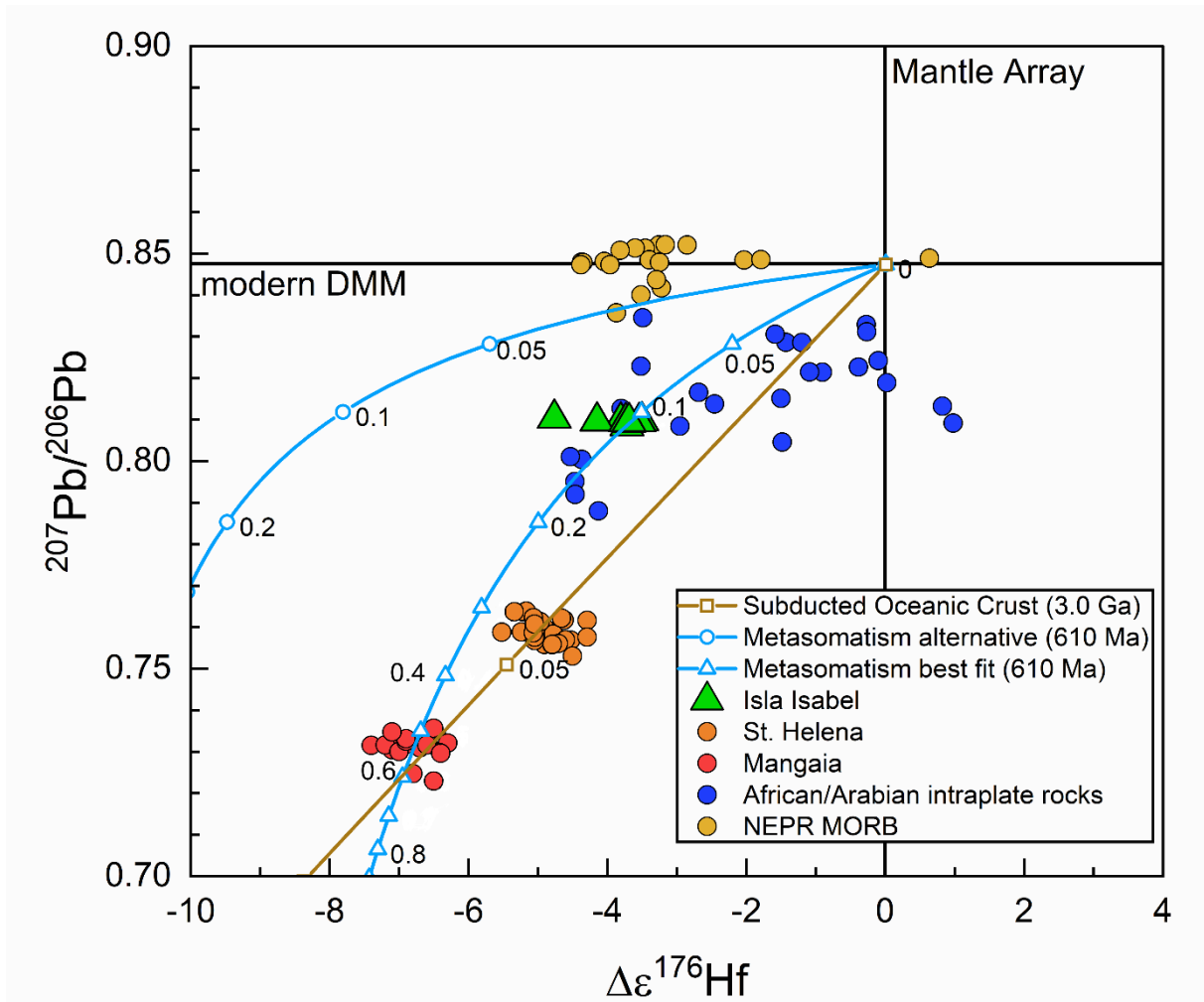
202



204 **Figure 1.** Map of the location of Isla Isabel, showing also relevant tectonic features (TF = Tamayo fault;
 205 SBF = San Blas fault; SBT = San Blas Trough; MMR = María Magdalena Rise). Cities (M = Mazatlán;
 206 SB = San Blas; TE = Tepic; G = Guadalajara; PV = Puerto Vallarta) and volcanoes of the western
 207 TMVB (SJ = San Juan; Sa = Sangangüey; Te = Tepetitlic; Ce = Ceboruco; Teq = Tequila; LP = Sierra
 208 La Primavera) are shown. The blue point on the inset map is the island Guadalupe. Features shown have
 209 been adapted from Housh et al. (2010), bathymetry grid data obtained from GEBCO
 210 (<https://www.gebco.net/>) (GEBCO Compilation Group, 2021).



213 **Figure 1.** Isotope composition of Isla Isabel lavas. a) $^{87}\text{Sr}/^{86}\text{Sr}$ vs $\epsilon^{143}\text{Nd}$, b) $^{206}\text{Pb}/^{204}\text{Pb}$ vs $^{207}\text{Pb}/^{204}\text{Pb}$,
 214 c) $^{208}\text{Pb}^*/^{206}\text{Pb}^*$ vs $^{87}\text{Sr}/^{86}\text{Sr}$, the $^{208}\text{Pb}^*/^{206}\text{Pb}^*$ ratio is calculated as described in Stracke et al., 2005, d)
 215 $\epsilon^{143}\text{Nd}$ vs $\epsilon^{176}\text{Hf}$ with mantle array according to Chauvel et al. (2008). For comparison, isotopic data
 216 from MORB, HIMU OIB, TMVB (intraplate lavas, where available), and African-Arabian intraplate
 217 rocks are plotted. Approximate compositions of OIB mantle components (DMM, HIMU, EM) are
 218 shown. The references for literature data are given in the Supplementary Information.



221 **Figure 2.** Mixing model for the $\Delta\epsilon^{176}\text{Hf}$ (deviation of the $\epsilon^{176}\text{Hf}$ compositions of a sample from the
 222 mantle array given the sample $\epsilon^{143}\text{Hf}$) versus $^{207}\text{Pb}/^{206}\text{Pb}$ compositions of DMM and metasomatized
 223 CLM compared to Isla Isabel and literature data. The blue lines represent the model mixing lines, for
 224 both best fit and alternative metasomatism models, as well as for a model for 3 Ga old recycled
 225 subducted oceanic crust (after Nebel et al. 2013). Symbols on the mixing lines represent the fraction
 226 metasomatized CLM component added. Comparison data are the same as in **Fig. 2.**

227

228 **References**

- 229 Aranda-Gómez, J.J., Luhr, J.F., Housh, T.B., Valdez-Moreno, G., and Chávez-Cabello, G., 2007, Late
230 Cenozoic intraplate-type volcanism in central and northern México: A review, in *Geology of*
231 *México: Celebrating the Centenary of the Geological Society of México*, Geological Society
232 of America, doi:10.1130/2007.2422(04).
- 233 Arevalo, R., and McDonough, W.F., 2010, Chemical variations and regional diversity observed in
234 MORB: *Chemical geology*, v. 271, p. 70–85, doi:10.1016/j.chemgeo.2009.12.013.
- 235 Ballentine, C.J., Lee, D.-C., and Halliday, A.N., 1997, Hafnium isotopic studies of the Cameroon line
236 and new HIMU paradoxes: *Chemical geology*, v. 139, p. 111–124, doi:10.1016/S0009-
237 2541(97)00028-4.
- 238 Brandenburg, J.P., Hauri, E.H., van Keken, P.E., and Ballentine, C.J., 2008, A multiple-system study
239 of the geochemical evolution of the mantle with force-balanced plates and thermochemical
240 effects: *Earth and planetary science letters*, v. 276, p. 1–13, doi:10.1016/j.epsl.2008.08.027.
- 241 Cabral, R.A., Jackson, M.G., Koga, K.T., Rose-Koga, E.F., Hauri, E.H., Whitehouse, M.J., Price,
242 A.A., Day, J.M.D., Shimizu, N., and Kelley, K.A., 2014, Volatile cycling of H₂O, CO₂, F,
243 and Cl in the HIMU mantle: A new window provided by melt inclusions from oceanic hot
244 spot lavas at Mangaia, Cook Islands: *Geochemistry, Geophysics, Geosystems*, v. 15, p. 4445–
245 4467, doi:10.1002/2014GC005473.
- 246 Chauvel, C., Goldstein, S.L., and Hofmann, A.W., 1995, Hydration and dehydration of oceanic crust
247 controls Pb evolution in the mantle: *Chemical Geology*, v. 126, p. 65–75, doi:10.1016/0009-
248 2541(95)00103-3.
- 249 Chauvel, C., Lewin, E., Carpentier, M., Arndt, N.T., and Marini, J.-C., 2008, Role of recycled oceanic
250 basalt and sediment in generating the Hf–Nd mantle array: *Nature Geoscience*, v. 1, p. 64–67,
251 doi:10.1038/ngeo.2007.51.
- 252 Cordier, C., Delavault, H., and Chauvel, C., 2021, Geochemistry of the Society and Pitcairn-Gambier
253 mantle plumes: What they share and do not share: *Geochimica et Cosmochimica Acta*, v. 306,
254 p. 362–384, doi:10.1016/j.gca.2021.04.014.
- 255 Díaz-Bravo, B.A., Gómez-Tuena, A., Ortega-Obregón, C., and Pérez-Arvizu, O., 2014, The origin of
256 intraplate magmatism in the western Trans-Mexican Volcanic Belt: *Geosphere*, v. 10, p. 340–
257 373, doi:10.1130/ges00976.1.
- 258 Engebretson, D.C., Cox, A., and Gordon, R., G., 1985, *Relative Motions Between Oceanic and*
259 *Continental Plates in the Pacific Basin*: Geological Society of America,
260 [https://pubs.geoscienceworld.org/gsa/books/book/330/Relative-Motions-Between-Oceanic-](https://pubs.geoscienceworld.org/gsa/books/book/330/Relative-Motions-Between-Oceanic-and-Continental)
261 [and-Continental](https://pubs.geoscienceworld.org/gsa/books/book/330/Relative-Motions-Between-Oceanic-and-Continental) (accessed September 2023).
- 262 Ferrari, L., Orozco-Esquivel, T., Manea, V., and Manea, M., 2012, The dynamic history of the Trans-
263 Mexican Volcanic Belt and the Mexico subduction zone: *Tectonophysics*, v. 522–523, p. 122–
264 149, doi:10.1016/j.tecto.2011.09.018.
- 265 GEBCO Compilation Group, 2021, GEBCO 2021 Grid:, doi:10.5285/c6612cbe-50b3-0cff-e053-
266 6c86abc09f8f.
- 267 Herzberg, C., Cabral, R.A., Jackson, M.G., Vidito, C., Day, J.M.D., and Hauri, E.H., 2014, Phantom
268 Archean crust in Mangaia hotspot lavas and the meaning of heterogeneous mantle: *Earth and*
269 *planetary science letters*, v. 396, p. 97–106, doi:10.1016/j.epsl.2014.03.065.

- 270 Hoernle, K., Hauff, F., Werner, R., van den Bogaard, P., Gibbons, A.D., Conrad, S., and Müller, R.D.,
271 2011, Origin of Indian Ocean Seamount Province by shallow recycling of continental
272 lithosphere: *Nature Geoscience*, v. 4, p. 883–887, doi:10.1038/ngeo1331.
- 273 Hofmann, A.W., 2014, Sampling Mantle Heterogeneity through Oceanic Basalts: Isotopes and Trace
274 Elements, *in* *Treatise on Geochemistry*, Amsterdam, Elsevier, p. 67–101.
- 275 Homrighausen, S., Hoernle, K., Hauff, F., Geldmacher, J., Wartho, J.-A., van den Bogaard, P., and
276 Garbe-Schönberg, D., 2018, Global distribution of the HIMU end member: Formation through
277 Archean plume-lid tectonics: *Earth-Science Reviews*, v. 182, p. 85–101,
278 doi:10.1016/j.earscirev.2018.04.009.
- 279 Housh, T.B., Aranda-Gómez, J.J., and Luhr, J.F., 2010, Isla Isabel (Nayarit, México): Quaternary
280 alkalic basalts with mantle xenoliths erupted in the mouth of the Gulf of California: *Journal of*
281 *Volcanology and Geothermal Research*, v. 197, p. 85–107,
282 doi:10.1016/j.jvolgeores.2009.06.011.
- 283 Jackson, M.G., Becker, T.W., and Konter, J.G., 2018, Evidence for a deep mantle source for EM and
284 HIMU domains from integrated geochemical and geophysical constraints: *Earth and Planetary*
285 *Science Letters*, v. 484, p. 154–167, doi:10.1016/j.epsl.2017.11.052.
- 286 Keppie, J.D., and Ortega-Gutiérrez, F., 2010, 1.3–0.9 Ga Oaxaquia (Mexico): Remnant of an
287 arc/backarc on the northern margin of Amazonia: *Journal of South American Earth Sciences*,
288 v. 29, p. 21–27, doi:10.1016/j.jsames.2009.07.001.
- 289 Koppers, A.A.P., Becker, T.W., Jackson, M.G., Konrad, K., Müller, R.D., Romanowicz, B.,
290 Steinberger, B., and Whittaker, J.M., 2021, Mantle plumes and their role in Earth processes:
291 *Nature Reviews Earth & Environment*, v. 2, p. 382–401, doi:10.1038/s43017-021-00168-6.
- 292 Lonsdale, P., 1991, Structural patterns of the Pacific floor offshore of Peninsular California., *in*
293 Dauphin, J.P. and Simoneit, B.R.T. eds., *Memoir 47: The Gulf and Peninsular Province of the*
294 *Californias*, Tulsa, OK, American Association of Petroleum Geology, p. 87–125.
- 295 McCoy-West, A.J., Bennett, V.C., and Amelin, Y., 2016, Rapid Cenozoic ingrowth of isotopic
296 signatures simulating “HIMU” in ancient lithospheric mantle: Distinguishing source from
297 process: *Geochimica et Cosmochimica Acta*, v. 187, p. 79–101,
298 doi:10.1016/j.gca.2016.05.013.
- 299 Mora-Klepeis, G., 2021, Mexico and the Gulf of Mexico, *in* *Encyclopedia of Geology*, p. 68–79.
- 300 Nebel, O., Arculus, R.J., van Westrenen, W., Woodhead, J.D., Jenner, F.E., Nebel-Jacobsen, Y.J.,
301 Wille, M., and Eggins, S.M., 2013, Coupled Hf–Nd–Pb isotope co-variations of HIMU
302 oceanic island basalts from Mangaia, Cook-Austral islands, suggest an Archean source
303 component in the mantle transition zone: *Geochimica et Cosmochimica Acta*, v. 112, p. 87–
304 101, doi:10.1016/j.gca.2013.03.005.
- 305 Rooney, T.O., Nelson, W.R., Dosso, L., Furman, T., and Hanan, B., 2014, The role of continental
306 lithosphere metasomes in the production of HIMU-like magmatism on the northeast African
307 and Arabian plates: *Geology*, v. 42, p. 419–422, doi:10.1130/g35216.1.
- 308 Salters, V.J.M., and Stracke, A., 2004, Composition of the depleted mantle: *Geochemistry,*
309 *Geophysics, Geosystems*, v. 5, p. p.n/a, doi:10.1029/2003gc000597.
- 310 Salters, V.J.M., and White, W.M., 1998, Hf isotope constraints on mantle evolution: *Chemical*
311 *Geology*, v. 145, p. 447–460, doi:10.1016/S0009-2541(97)00154-X.

- 312 Smith, A.D., 1999, The Nd-Sr-Pb Isotopic Record in Abyssal Tholeiites from the Gulf of California
313 Region, Western Mexico: No Evidence for a Gulf Mouth Plume: *International Geology*
314 *Review*, v. 41, p. 921–931, doi:10.1080/00206819909465179.
- 315 Stracke, A., Hofmann, A.W., and Hart, S.R., 2005, FOZO, HIMU, and the rest of the mantle zoo:
316 *Geochemistry, Geophysics, Geosystems*, v. 6, p. Q05007- n/a, doi:10.1029/2004gc000824.
- 317 Weiss, Y., Class, C., Goldstein, S., and Hanyu, T., 2016, Key new pieces of the HIMU puzzle from
318 olivines and diamond inclusions: *Nature*, v. 537, p. 666–670, doi:10.1038/nature19113.
- 319 Wittig, N., Pearson, D.G., Duggen, S., Baker, J., and Hoernle, K., 2010, Tracing the metasomatic and
320 magmatic evolution of continental mantle roots with Sr, Nd, Hf and and Pb isotopes: A case
321 study of Middle Atlas (Morocco) peridotite xenoliths: *Geochimica et Cosmochimica Acta*, v.
322 74, p. 1417–1435, doi:10.1016/j.gca.2009.10.048.
- 323 Workman, R.K., and Hart, S.R., 2005, Major and trace element composition of the depleted MORB
324 mantle (DMM): *Earth and planetary science letters*, v. 231, p. 53–72,
325 doi:10.1016/j.epsl.2004.12.005.
- 326 Zindler, A., and Hart, S.R., 1986, *Chemical Geodynamics: Annual review of earth and planetary*
327 *sciences*, v. 14, p. 493–571, doi:10.1146/annurev.ea.14.050186.002425.

328

329

330

331

1
2
3
4
5
6
7
8

Supplementary information and figures for:

Pre-Cordilleran mantle metasomatism preserved in alkali basalts of Isla Isabel, México

Leonie Sieger, Bradley J. Peters, Andrea Giuliani, Maria Schönbächler
Institute of Geochemistry and Petrology, ETH Zürich, CH-8092 Zürich, Switzerland

*Submitted to *Geology**

This is a non-peer reviewed preprint uploaded to EarthArXiv

1. Methods

The nine analyzed Isla Isabel samples are the same as in Housh et al. (2010) and were provided by the Smithsonian Museum of Natural History. The GPS coordinates for sample collection locations are provided in Table 1 of Housh et al. (2010) and replicated in **Table S1**. Housh et al. (2010) only reported isotopic data for four samples and no Hf isotopic data. All sample powders, except for that for BHVO-2, were repetitively leached with 2M HCl in an ultrasonic bath in 20-minute intervals. After each leaching interval, the acid and all suspended fine particles were removed with a pipette. The leaching was repeated until the acid solution remained transparent after the 20-minute ultrasonication. At this point, the leachate was again removed, and the leach was stopped by adding mQ H₂O to the sample and ultrasonicing the sample for a further 20 minutes. Subsequently, the H₂O was decanted from the sample with a pipette and the sample residues were gently dried. They were subsequently digested in a 4:1 mixture of concentrated, distilled HF and concentrated, double-distilled HNO₃ for >3 days.

The separation method for Hf was adapted from Münker et al. (2001) and completed on a separate aliquot from the same sample digestion used for Sr-Nd-Pb separations. First, high field strength elements (HFSE), including Hf, were separated from matrix elements in 1M HCl-0.1M HF on BioRad AG50-X8, 200-400 mesh cation exchange resin. The sample aliquots were then dried and repetitively dissolved in drops of concentrated, high-purity HClO₄ to oxidize Ti. Following this, Hf was separated from other HFSE on 50-100 µm Eichrom Ln resin. The Hf collection procedure was calibrated, which was accomplished using the basaltic reference material BCR-2. This second column step encompasses separation of Ti (in 0.09M HCl-0.45M HNO₃-1 wt% H₂O₂) and Zr (in 2M HCl-0.1M HF) and finally the collection of Hf isotopes using 6M HCl-0.04M HF. Lead was separated from matrix elements using BioRad AG1-X8 anion exchange resin using 0.5N HBr (matrix) and 0.5M HNO₃ (Pb). Following this, Nd was separated from the Pb matrix fraction in two steps using BioRad AG50-X8, 200-400 mesh cation exchange resin and 50-100 µm Eichrom Ln resin. Strontium was separated from the sample matrix on Eichrom Sr resin using the matrix fraction collected in the first step of Nd separation.

The Nd, Hf, and Pb isotopic compositions of the Isla Isabel samples were measured using the Thermo Scientific Neptune multi-collector inductively coupled plasma source mass spectrometry (MC-ICP-MS) in the Isotope Geochemistry and Cosmochemistry group at ETH Zürich. Neodymium isotopic compositions were normalized to $^{146}\text{Nd}/^{144}\text{Nd} = 0.7219$ and $^{142}\text{Nd}/^{144}\text{Nd} = 1.141876$ using a $^{142}\text{Ce}/^{140}\text{Ce}$ ratio that was empirically calculated from the offset in fractionation-corrected $^{143}\text{Nd}/^{144}\text{Nd}$ ratios between the JNdi-1 standard with and without an added Ce dopant. The corrected $^{143}\text{Nd}/^{144}\text{Nd}$ ratios were then normalized to a reference JNdi-1 $^{143}\text{Nd}/^{144}\text{Nd}$ value of 0.512115 (Tanaka et al., 2004) on a per-session basis. Hafnium isotopic compositions were normalized to $^{179}\text{Hf}/^{177}\text{Hf} = 0.7325$ and corrected $^{177}\text{Hf}/^{176}\text{Hf}$ ratios were normalized to a reference value of 0.282160 for the JMC475 standard (Blichert-Toft et al., 1997). Lead isotopic compositions were corrected for mass bias using Tl doping and a $^{203}\text{Tl}/^{205}\text{Tl}$ ratio calculated to produce a total offset of zero between measured $^{206,207,208}\text{Pb}/^{204}\text{Pb}$ and $^{207,208}\text{Pb}/^{206}\text{Pb}$ ratios and the reference values of Baker et al. (2004). External precisions (estimated as the 2σ s.d. of all measured standards in one measurement session) were 0.06-0.09 for $\epsilon^{143}\text{Nd}$ (two measurement sessions), 0.24 for $\epsilon^{176}\text{Hf}$ (one measurement session), 0.0009-0.0010 for $^{206}\text{Pb}/^{204}\text{Pb}$, 0.0008-0.0012 for $^{207}\text{Pb}/^{204}\text{Pb}$, and 0.0020-0.0032 for $^{208}\text{Pb}/^{204}\text{Pb}$ (three measurement sessions). The obtained isotopic compositions for BHVO-2 digested and processed with the Isla Isabel samples agree with literature reference values (**Table 1**).

Strontium isotopic compositions were measured using the Thermo Scientific Triton thermal ionization mass spectrometer (TIMS) in the Isotope Geochemistry and Cosmochemistry group at ETH Zürich. The data were normalized to $^{88}\text{Sr}/^{86}\text{Sr} = 8.375209$ and the corrected $^{87}\text{Sr}/^{86}\text{Sr}$ values were normalized to a reference $^{87}\text{Sr}/^{86}\text{Sr}$ ratio of 0.710245 for the NBS987 standard (mean of published values on the GeoREM database). The external precision for $^{87}\text{Sr}/^{86}\text{Sr}$ ratios, estimated as the s.d. of all measured standards, was 0.000009. Measured isotopic compositions for BHVO-2 digested and chemically separated with the Isla Isabel samples agree with literature reference values (**Table 1**).

For all samples and isotopic systems, uncertainties of single measurements are expressed as the larger of (i) the 2σ standard error of the measurement and (ii) the 2σ standard deviation of all measured standards as reported in the sections above. The reported values and uncertainties of replicated standard

61 and sample measurements are the weighted average and 2σ standard deviation of individual runs,
62 weighted by the uncertainty of individual measurements as previously defined.

63

64 2. Model age calculations

65 The timing of the metasomatic event that generated the Nd-Hf-Pb isotopic signatures associated with
66 HIMU OIB can be constrained with the help of the Lu-Hf and Sm-Nd isotopic systems, and through this
67 potentially linked to tectonic or magmatic events. To determine the age constraints for the model
68 calculations, the closing time of the systems τ was calculated based on the collected isotope data. Since
69 the Lu-Hf isotope system experiences very small amounts of fractionation between parent and daughter
70 elements during partial melting of intraplate basalts from metasomatized mantle, measured Lu/Hf ratios
71 of the rocks are assumed to be the same as in the magma source (cf., Pilet et al., 2008; Rooney et al.,
72 2014):

$$73 \tau_{176} = \frac{1}{\lambda} * \ln \left(\frac{\frac{^{176}\text{Hf}}{^{177}\text{Hf}}_{\text{sample}} - \frac{^{176}\text{Hf}}{^{177}\text{Hf}}_{\text{DMM}}}{\frac{^{176}\text{Lu}}{^{177}\text{Hf}}_{\text{sample}} - \frac{^{176}\text{Lu}}{^{177}\text{Hf}}_{\text{DMM}}} + 1 \right)$$

74

75 The average τ_{176} value based on the Isla Isabel isotope data is $\tau_{176} = 616 \pm 35$ Ma. The same calculations
76 for the Sm-Nd system result in a younger age of $\tau_{143} = 376 \pm 27$ Ma, both of which reflect pre-Cordilleran
77 ages. The average τ_{143} age is somewhat older than the age of mantle metasomatism inferred from the Nd
78 isotopic compositions of mantle xenoliths in northwest México, approximately 700 km NNE of Isla
79 Isabel (<227 Ma; Nimz et al., 1995). The difference in the ages implied by the two isotope systems is
80 likely related to differences in the closed system behavior of Hf isotopes compared to Nd isotopes. It
81 has been observed that although the two isotope systems have similar compatibility behaviors, among
82 mantle lithologies the Sm-Nd system seems to be more sensitive to later-stage disturbances, like melt-
83 rock interactions, than the Lu-Hf system (Stracke et al., 2011). Thus, the Lu-Hf system is considered the
84 more robust indicator of the timing of the metasomatic or other enrichment event affecting the Isla Isabel
85 mantle source. A geologically parsimonious explanation for the differing model ages is that they reflect
86 distinct events that affected the Sm-Nd and Lu-Hf systems differently. For example, the >735 Ma mantle
87 depletion age inferred from the least metasomatized mantle xenoliths of Nimz et al. (1995, from
88 northwest México ca. 700 km NNE of Isla Isabel), along with the average Hf depletion age of Isla Isabel
89 samples (616 Ma) may reflect collision-rifting cycles associated with the supercontinent Rodinia (e.g.,
90 Keppie and Ortega-Gutiérrez, 2010). The Paleozoic Nd model ages of the northwest México mantle
91 xenoliths (Nimz et al., 1995) and the Isla Isabel samples may reflect distinct episodes of smaller-scale
92 magmatism that are recorded for example in the Coahuila terrane of northwestern México and the
93 southern United States (e.g., Denison et al., 1969).

94 It is important to note that these model ages do not necessarily directly reflect the time at which the
95 regional continental lithospheric mantle (CLM) was metasomatized, since they reflect the measured
96 $\varepsilon^{176}\text{Hf}$ and Lu/Hf ratios of the samples, which represent the composition mixed mantle source (DMM +
97 CLM) and not the composition of the metasomatic CLM component itself. Since the $\Delta\varepsilon^{176}\text{Hf}$
98 composition of Isla Isabel basalts is a mixture of depleted mantle ($\Delta\varepsilon^{176}\text{Hf}$ near 0) and the metasomatized
99 component, the latter must have a $\Delta\varepsilon^{176}\text{Hf}$ composition that is more negative than Isla Isabel. More
100 negative $\Delta\varepsilon^{176}\text{Hf}$ signatures would require more time to evolve from a pre-metasomatic peridotite that
101 is DMM-like compared to less negative $\Delta\varepsilon^{176}\text{Hf}$ signatures, unless the Lu/Hf ratio of the more negative
102 $\Delta\varepsilon^{176}\text{Hf}$ domain is low enough to allow the negative $\Delta\varepsilon^{176}\text{Hf}$ signatures to develop in a shorter time. For
103 example, Woodhead et al. (2017) reported Hf isotopic data for a global assemblage of mantle-derived
104 zircon, which, due to their very low Lu/Hf ratios and relatively young ages (<120 Ma), preserve their
105 initial Hf compositions. Within their “group A,” in which Hf isotopic compositions are correlated with
106 age, a kernel density estimate reveals a peak $\varepsilon^{176}\text{Hf}$ composition of ca. -3. Assuming the most extreme
107 case of Lu/Hf = 0, which will produce the youngest possible τ_{176} age, if the metasomatized CLM
108 contributing to the Isla Isabel source possessed a $\varepsilon^{176}\text{Hf}$ of -3, its τ_{176} would be ca. 750 Ma. In the most

109 extreme possible example for Isla Isabel, a metasomatized CLM source with Lu/Hf = 0 and $\epsilon^{176}\text{Hf} \approx$
110 $+0.4$ would produce a τ_{176} virtually identical to the average τ_{176} of the samples. However, this would
111 require that the metasomatized CLM contributes ca. 55% of the Hf budget of Isla Isabel basalts. Such a
112 high proportion would more likely produce a more volatile-rich mafic lithology, approaching a lamproite
113 or a carbonatite, than the alkali basalts that characterize Isla Isabel. The Isla Isabel samples would also
114 likely possess trace element characteristics that are common in these rock types, such as enrichments in
115 Th and Ba (e.g., Hoernle et al., 2002), which are absent in the Isla Isabel basalts. Thus, utilizing the
116 Lu/Hf ratios of the Isla Isabel samples to calculate the age of CLM metasomatism likely underestimates
117 the age of regional CLM metasomatism. There are no regional constraints on the Lu/Hf and ratio of the
118 CLM that would permit the model to be constructed otherwise, however mantle xenoliths from
119 northwestern México (ca. 700 km NNE of Isla Isabel; Nimz et al., 1995) similarly preserve a pre-
120 Cordilleran model age of >735 Ma in their Nd model ages. Further, there are no direct constraints on
121 the U,Pb/Th ratios or Pb isotopic compositions of the regional lithospheric mantle that could be used to
122 complete the model into its form in **Fig. 3**.

123

124 **3. Model fitting of the metasomatized component**

125 Determining the starting composition of the enriched component of the Isla Isabel magma source is
126 difficult as combined data for the Sm-Nd, Lu-Hf, and U,Th-Pb isotopic systems is relatively scarce for
127 lithospheric mantle xenoliths. Compositions able to generate the required isotope compositions can be
128 found by model fitting and using literature data for global xenoliths of CLM. For the Pb isotope
129 compositions, a $^{238}\text{U}/^{204}\text{Pb}$ of 56.3 (Wittig et al., 2010) observed in metasomatized continental mantle
130 xenoliths reproduce the isotopic compositions of Isla Isabel lavas assuming a starting age of 616 Ma
131 (i.e. the average Lu-Hf model age of the samples). However, the Lu/Hf and Sm/Nd ratios of the same
132 rocks are not able to reproduce the observed Nd and Hf isotopic compositions of Isla Isabel lavas;
133 instead, the component requires a more enriched Lu/Hf ratio compared to the depleted mantle than the
134 enrichment of Sm/Nd ratios compared to the depleted mantle. This incongruous enrichment can be
135 observed in the same metasomatized mantle samples from Wittig et al. (2010), but the enrichment is not
136 extreme enough (e.g., $^{176}\text{Lu}/^{177}\text{Hf} = 0.02$ and $^{147}\text{Sm}/^{144}\text{Nd} = 0.21$; Wittig et al., 2010) to produce Nd-Hf
137 isotopic compositions as far below the mantle array as what is observed for Isla Isabel lavas. In order to
138 produce a fit to the Isla Isabel data, the Lu/Hf ratio of their most extreme sample was thus adjusted
139 downwards, and its Sm/Nd ratio was proportionally adjusted upwards. This represents an artificial
140 arithmetic adjustment; however, it mimics the same metasomatic enrichment process observed in the
141 samples of Wittig et al. (2010), but to a higher degree.

142 The best fit mixing line for the Isla Isabel samples also passes through samples from Gerba Guracha,
143 which have been suggested to originate from melting of amphibole-rich lithospheric metasomes,
144 resulting in their HIMU-like compositions (Rooney et al., 2014). Isla Isabel samples have similar
145 $^{207}\text{Pb}/^{206}\text{Pb}$ and $\Delta\epsilon^{176}\text{Hf}$ values to the lavas from Gerba Guracha (Fig. 2), which speaks for the possibility
146 of a similar metasomatic component being involved in the island's magma source.

147

148

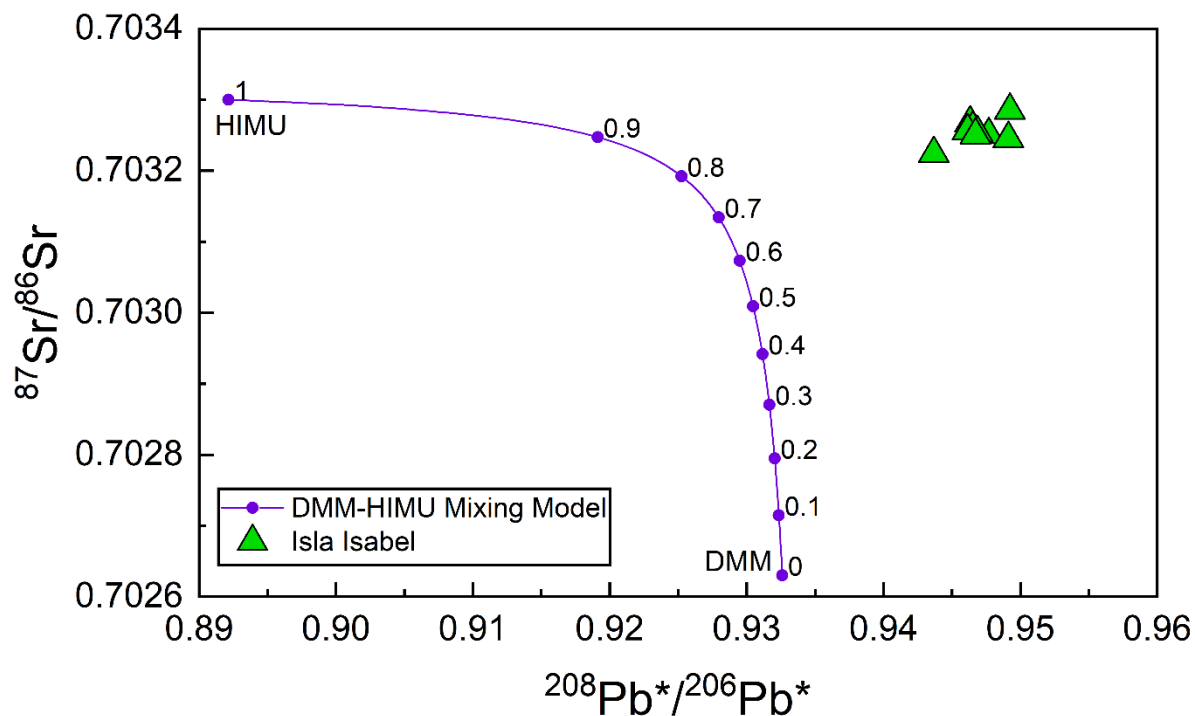
149 **Supplementary table and figures**

150 **Supplementary Table S1.** GPS collection coordinates for samples used in this study.

Sample	Latitude	Longitude
NAY-2	21.8436	-105.8794
NAY-3	21.8436	-105.8794
NAY-4	21.8500	-105.8878
NAY-13	21.8463	-105.8844
NAY-14	21.8491	-105.8851
NAY-15	21.8492	-105.8888
NAY-31	21.8480	-105.8879
NAY-32	21.8433	-105.8864
NAY-35	21.8445	-105.8861

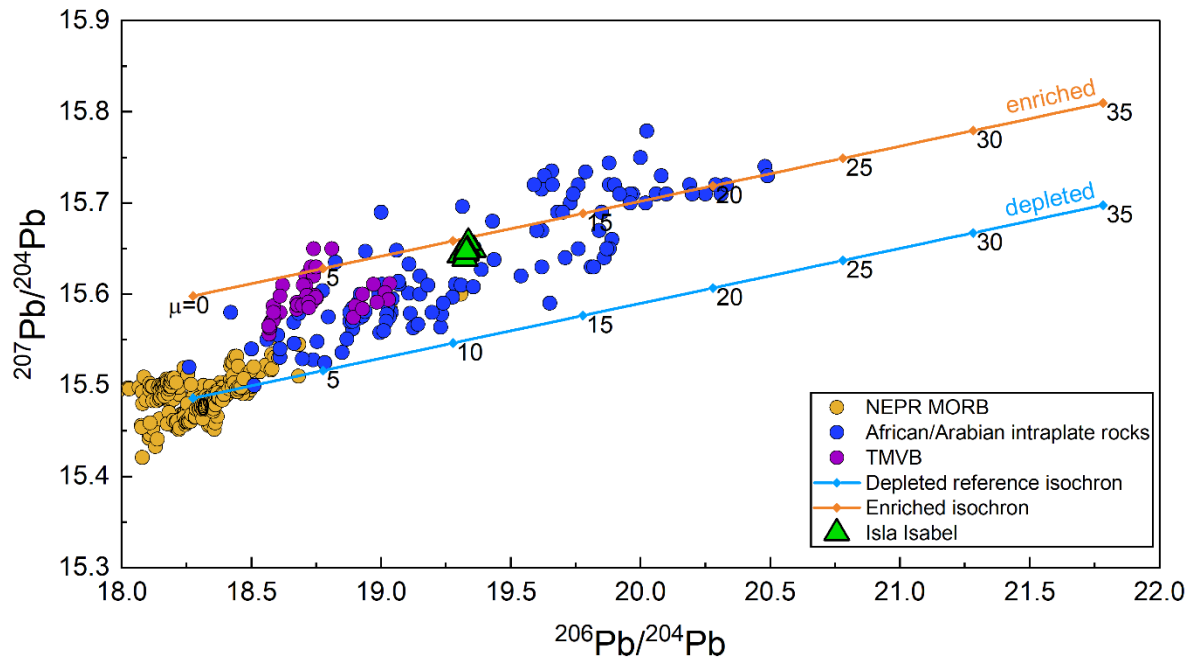
151

152



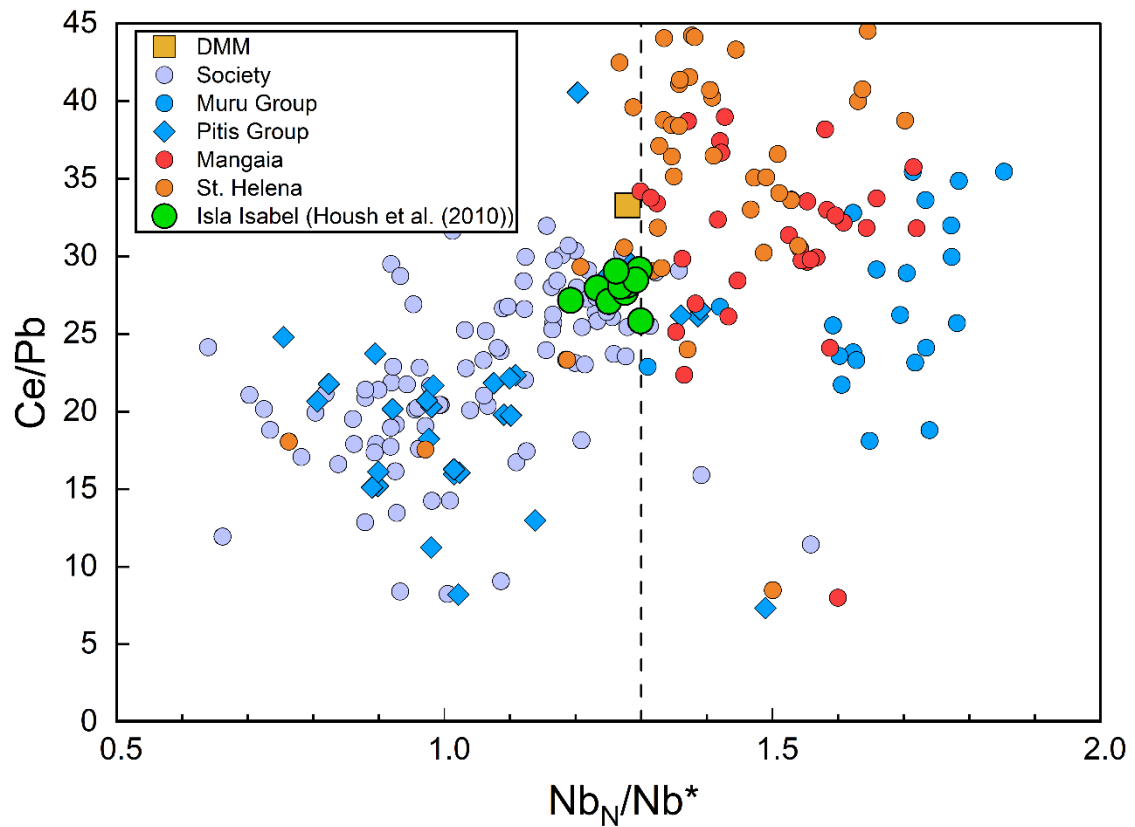
153

154 **Supplementary Figure S1.** $^{87}\text{Sr}/^{86}\text{Sr}$ versus $^{208}\text{Pb}^*/^{206}\text{Pb}^*$ non-linear isotope mixing model. Points and
 155 numbers indicate the fraction of HIMU component in the mixture. This simple model indicates that
 156 mixing between enriched (e.g., HIMU component originating from recycled subducted oceanic crust)
 157 and a depleted (e.g., DMM) endmembers is unable to produce Isla Isabel isotope compositions.
 158 Endmember isotopic compositions are derived from the literature (DMM: $^{87}\text{Sr}/^{86}\text{Sr} = 0.7026$, $^{206}\text{Pb}/^{204}\text{Pb}$
 159 $= 18.23$, $^{208}\text{Pb}/^{204}\text{Pb} = 37.84$, Workman and Hart, 2005; HIMU: $^{87}\text{Sr}/^{86}\text{Sr} = 0.7033$, $^{206}\text{Pb}/^{204}\text{Pb} = 22$,
 160 $^{208}\text{Pb}/^{204}\text{Pb} = 40.8$, Stracke et al., 2005). The choice of Pb and Sr elemental abundances in the mixing
 161 model is arbitrary, since there is no possible mixing line that would pass through the Isla Isabel data; the
 162 displayed mixing line is thus only illustrative.



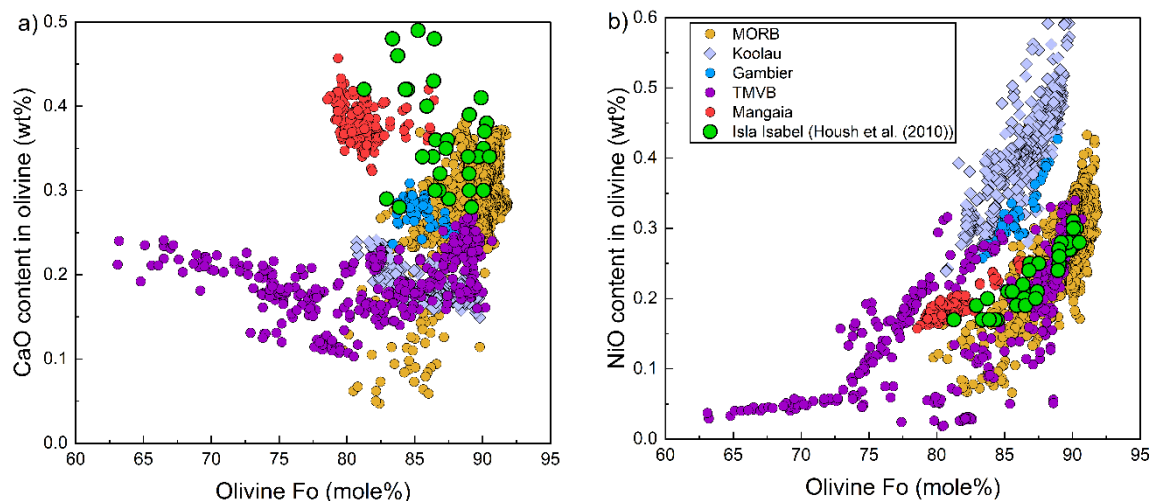
163

164 **Supplementary Figure S2.** Isotope model of $^{207}\text{Pb}/^{204}\text{Pb}$ versus $^{206}\text{Pb}/^{204}\text{Pb}$ isochrons adapted from
 165 Rooney et al. (2014). The model compares the evolution of Pb-Pb isochrons with varying μ values at a
 166 fixed time (ca. 600 Ma) based on the Isla Isabel Hf isotope data (τ_{176}). The reference depleted isochron
 167 starts with an initial composition representing DMM Pb isotope signatures (Workman and Hart, 2005)
 168 using μ ranges from 0-35. This isochron lies below the Isla Isabel data. The adjusted, enriched isochron
 169 is fitted to the most extreme Isla Isabel value by increasing the initial value of $^{207}\text{Pb}/^{204}\text{Pb}$ from 15.486
 170 to 15.598. This increase could represent a geochemical enrichment event affecting DMM material,
 171 generated for example by incorporation of subducted oceanic crust or metasomatized CLM. Along with
 172 the Isla Isabel samples, intraplate rocks that have metasomatized mantle sources are plotted for
 173 reference. Together, they illustrate a broad mixing line between the two isochrons.



174

175 **Supplementary Figure S3.** Ce/Pb versus Nb_N/Nb^* ($Nb_{PM} / (La_{PM} * Th_{PM})^{1/2}$, where PM indicates
 176 normalization to the primitive mantle composition of McDonough & Sun, 1995) for Isla Isabel and
 177 comparison data from literature. These trace element ratios can be used to infer information about the
 178 sources of intraplate magmas because they are relatively unaffected by partial melting and fractional
 179 crystallization and have distinct values in continental crust and mantle material. Trace element
 180 compositions of Isla Isabel (Housh et al., 2010) overall overlap with depleted mantle values (22 ± 10 ;
 181 Arevalo and McDonough, 2010), while classical HIMU rocks such as Mangaia and St. Helena, which
 182 are thought to derive from recycled, subducted oceanic crust and tend to have high Nb_N/Nb^* and Ce/Pb
 183 values (Cordier et al., 2021). The vertical dashed line represents the boundary between the Pitlis
 184 (depleted) and Muru (recycled) group lavas within the Pitcairn-Gambier hotspot chain, as proposed by
 185 Cordier et al. (2021). The lack of strongly elevated Ce/Pb and Nb_N/Nb^* ratios, producing a dissimilarity
 186 with the Muru group, indicates that a classical HIMU origin is unlikely for the Isla Isabel isotope
 187 composition.



188

189 **Supplementary Figure S4.** Olivine compositions of Isla Isabel (Housh et al., 2010) compared to
 190 literature data: a) CaO versus forsterite (Fo) content; b) NiO versus forsterite content. Isla Isabel olivines
 191 have low NiO and high CaO contents, overlapping with both olivines from MORB (Sobolev et al., 2007)
 192 and the TMVB (Díaz-Bravo et al., 2014). These data are consistent with derivation of Isla Isabel lavas
 193 from partial melting of peridotite source (e.g., high CaO, low NiO; Díaz-Bravo et al., 2014). The
 194 recycling of oceanic crust tends to generate hybrid pyroxenite mantle lithologies, which produce low
 195 CaO, high NiO olivines when melted, as observed in the Ko‘olau (Hawai‘i) and Gambier (French
 196 Polynesia) olivines. The lack of evidence for a pyroxenite component in the Isla Isabel olivine
 197 compositions argues against derivation of Isla Isabel lavas from recycled oceanic crust, and rather
 198 implies the involvement of metasomatized mantle lithologies, for example with carbonatitic melts
 199 (McCoy-West et al., 2016; Weiss et al., 2016).

200

201 Literature data

202 For comparison with the Isla Isabel data, literature values from lavas of different locations and origin
 203 were plotted.

204 Figures 2, 3, and S2: MORB (Castillo et al., 2000; Niu et al., 2002; Debaille et al., 2006; Waters et al.,
 205 2011; Mougél et al., 2014; Mallick et al., 2019), TMVB (Pier et al., 1992; Petrone et al., 2003; Valdez-
 206 Moreno et al., 2006; Díaz-Bravo et al., 2014), African and Arabian intraplate rocks (Bertrand et al.,
 207 2003; Lucassen et al., 2008; Rooney et al., 2014), St. Helena (Hanyu et al., 2014) and Mangaia
 208 (Woodhead, 1996; Nebel et al., 2013)

209 Supplementary Figure S3: DMM (Salters and Stracke, 2004), Pacific islands (Cordier et al., 2021), St.
 210 Helena (DIGIS Team, 2021), Mangaia (DIGIS Team, 2021), Isla Isabel (Housh et al., 2010)

211 Supplementary Figure S4: MORB (Sobolev et al., 2007), Koolau (Sobolev et al., 2007), Gambier
 212 (Delavault et al., 2015), TMVB (Díaz-Bravo et al., 2014), Mangaia (Herzberg et al., 2014), Isla Isabel
 213 (Housh et al., 2010)

214

215 Supplementary References

216 Arevalo, R., and McDonough, W.F., 2010, Chemical variations and regional diversity observed in
 217 MORB: *Chemical geology*, v. 271, p. 70–85, doi:10.1016/j.chemgeo.2009.12.013.

218 Baker, J., Peate, D., Waight, T., and Meyzen, C., 2004, Pb isotopic analysis of standards and samples
 219 using a ^{207}Pb - ^{204}Pb double spike and thallium to correct for mass bias with a double-focusing
 220 MC-ICP-MS. *Chemical Geology*, v. 211, p. 275-303, doi:10.1016/j.chemgeo.2004.06.030.

- 221 Bertrand, H., Chazot, G., Blichert-Toft, J., and Thoral, S., 2003, Implications of widespread high- μ
222 volcanism on the Arabian Plate for Afar mantle plume and lithosphere composition: *Chemical*
223 *geology*, v. 198, p. 47–61, doi:10.1016/S0009-2541(02)00418-7.
- 224 Blichert-Toft, J., and Albarède, F., 1997, the Lu-Hf isotope geochemistry of chondrites and the
225 evolution of the mantle-crust system. *Earth and Planetary Science Letters*, v. 148, p. 243-258,
226 doi:10.1016/S0012-821X(97)00040-X.
- 227 Castillo, P.R., Klein, E., Bender, J., Langmuir, C., Shirey, S., Batiza, R., and White, W., 2000,
228 Petrology and Sr, Nd, and Pb isotope geochemistry of mid-ocean ridge basalt glasses from the
229 11°45'N to 15°00'N segment of the East Pacific Rise: *Geochemistry, Geophysics,*
230 *Geosystems*, v. 1, doi:10.1029/1999gc000024.
- 231 Cordier, C., Delavault, H., and Chauvel, C., 2021, Geochemistry of the Society and Pitcairn-Gambier
232 mantle plumes: What they share and do not share: *Geochimica et Cosmochimica Acta*, v. 306,
233 p. 362–384, doi:10.1016/j.gca.2021.04.014.
- 234 Debaille, V., Blichert-Toft, J., Agraniér, A., Doucelance, R., Schiano, P., and Albarede. Francis, 2006,
235 Geochemical component relationships in MORB from the Mid-Atlantic Ridge, 22–35°N:
236 *Earth and planetary science letters*, v. 241, p. 844–862, doi:10.1016/j.epsl.2005.11.004.
- 237 Delavault, H., Chauvel, C., Sobolev, A., and Batanova, V., 2015, Combined petrological, geochemical
238 and isotopic modeling of a plume source: Example of Gambier Island, Pitcairn chain: *Earth*
239 *and planetary science letters*, v. 426, p. 23–35, doi:10.1016/j.epsl.2015.06.013.
- 240 Denison, R.E., Kenny, G.S., Burke, W.H., and Hetherington, E.A., 1969, Isotopic ages of igneous and
241 metamorphic boulders from the Haymond Formation (Pennsylvanian), Marathon Basin,
242 Texas, and their significance: *Geological Society of America Bulletin*, v. 80, p. 245-256, doi:
243 10.1130/0016-7606(1969)80[245:IAOIAM]2.0.CO;2.
- 244 Díaz-Bravo, B.A., Gómez-Tuena, A., Ortega-Obregón, C., and Pérez-Arvizu, O., 2014, The origin of
245 intraplate magmatism in the western Trans-Mexican Volcanic Belt: *Geosphere*, v. 10, p. 340–
246 373, doi:10.1130/ges00976.1.
- 247 DIGIS Team, 2021, GEOROC Compilation: Ocean Island Groups:, doi:10.25625/WFJZKY.
- 248 Hanyu, T. et al., 2014, Isotope evolution in the HIMU reservoir beneath St. Helena: Implications for
249 the mantle recycling of U and Th: *Geochimica et Cosmochimica Acta*, v. 143, p. 232–252,
250 doi:10.1016/j.gca.2014.03.016.
- 251 Herzberg, C., Cabral, R.A., Jackson, M.G., Vidito, C., Day, J.M.D., and Hauri, E.H., 2014, Phantom
252 Archean crust in Mangaia hotspot lavas and the meaning of heterogeneous mantle: *Earth and*
253 *planetary science letters*, v. 396, p. 97–106, doi:10.1016/j.epsl.2014.03.065.
- 254 Hoernle, K., Tilton, G., Le Bas, M.J., Duggen, S., and Garbe-Schönberg, D., 2002, Geochemistry of
255 oceanic carbonatites compared with continental carbonatites: mantle recycling of oceanic
256 crustal carbonate: *Contributions to Mineralogy and Petrology*, v. 142, p. 520-542,
257 doi:10.1007/s004100100308.
- 258 Housh, T.B., Aranda-Gómez, J.J., and Luhr, J.F., 2010, Isla Isabel (Nayarit, México): Quaternary
259 alkalic basalts with mantle xenoliths erupted in the mouth of the Gulf of California: *Journal of*
260 *Volcanology and Geothermal Research*, v. 197, p. 85–107,
261 doi:10.1016/j.jvolgeores.2009.06.011.
- 262 Lucassen, F., Franz, G., Romer, R.L., Pudlo, D., and Dulski, P., 2008, Nd, Pb, and Sr isotope
263 composition of Late Mesozoic to Quaternary intra-plate magmatism in NE-Africa (Sudan,

- 264 Egypt): high- μ signatures from the mantle lithosphere: Contributions to mineralogy and
265 petrology, v. 156, p. 765–784, doi:10.1007/s00410-008-0314-0.
- 266 Mallick, S., Salters, V.J., and Langmuir, C.H., 2019, Geochemical variability along the northern East
267 Pacific Rise: Coincident source composition and ridge segmentation: Geochemistry,
268 Geophysics, Geosystems, v. 20, p. 1889–1911, doi:10.1029/2019gc008287.
- 269 McCoy-West, A.J., Bennett, V.C., and Amelin, Y., 2016, Rapid Cenozoic ingrowth of isotopic
270 signatures simulating “HIMU” in ancient lithospheric mantle: Distinguishing source from
271 process: *Geochimica et Cosmochimica Acta*, v. 187, p. 79–101,
272 doi:10.1016/j.gca.2016.05.013.
- 273 McDonough, W.F., and Sun, S.-s., 1995, The composition of the Earth: *Chemical Geology*, v. 120, p.
274 223–253, doi:10.1016/0009-2541(94)00140-4.
- 275 Mougél, B., Agraniér, A., Hemond, C., and Gente, P., 2014, A highly unradiogenic lead isotopic
276 signature revealed by volcanic rocks from the East Pacific Rise: *Nature Communications*, v. 5,
277 p. 4474, doi:10.1038/ncomms5474.
- 278 Münker, C., Weyer, S., Scherer, E., and Mezger, K., 2001, Separation of high field strength elements
279 (Nb, Ta, Zr, Hf) and Lu from rock samples for MC-ICPMS measurements: *Geochemistry*,
280 *Geophysics, Geosystems*, v. 2, p. p.n/a, doi:10.1029/2001GC000183.
- 281 Nebel, O., Arculus, R.J., van Westrenen, W., Woodhead, J.D., Jenner, F.E., Nebel-Jacobsen, Y.J.,
282 Wille, M., and Eggins, S.M., 2013, Coupled Hf–Nd–Pb isotope co-variations of HIMU
283 oceanic island basalts from Mangaia, Cook-Austral islands, suggest an Archean source
284 component in the mantle transition zone: *Geochimica et Cosmochimica Acta*, v. 112, p. 87–
285 101, doi:10.1016/j.gca.2013.03.005.
- 286 Nimz, G.J., Cameron, K.L., and Niemeyer, S., 1995, Formation of mantle lithosphere beneath northern
287 Mexico: Chemical and Sr–Nd–Pb isotopic systematics of peridotite xenoliths from La Olivina:
288 *Journal of Geophysical Research*, v. 100, p. 4181–4196, doi: 10.1029/94JB02776.
- 289 Niu, Y., Regelous, M., Wendt, I.J., Batiza, R., and O’Hara, M.J., 2002, Geochemistry of near-EPR
290 seamounts: importance of source vs. process and the origin of enriched mantle component:
291 *Earth and planetary science letters*, v. 199, p. 327–345, doi:10.1016/S0012-821X(02)00591-5.
- 292 Petrone, C.M., Francalanci, L., Carlson, R.W., Ferrari, L., and Conticelli, S., 2003, Unusual
293 coexistence of subduction-related and intraplate-type magmatism: Sr, Nd and Pb isotope and
294 trace element data from the magmatism of the San Pedro–Ceboruco graben (Nayarit, Mexico):
295 *Chemical geology*, v. 193, p. 1–24, doi:10.1016/S0009-2541(02)00229-2.
- 296 Pier, J.G., Luhr, J.F., Podosek, F.A., and Aranda-Gómez, J.J., 1992, The La Breña - El Jagüey Maar
297 Complex, Durango, Mexico. II: Petrology and geochemistry: *Bulletin of volcanology*, v. 54, p.
298 405–428, doi:10.1007/BF00312322.
- 299 Pilet, S., Baker, M.B., and Stolper, E.M., 2008, Metasomatized Lithosphere and the Origin of Alkaline
300 Lavas: *Science*, v. 320, p. 916–919, doi:doi:10.1126/science.1156563.
- 301 Rooney, T.O., Nelson, W.R., Dosso, L., Furman, T., and Hanan, B., 2014, The role of continental
302 lithosphere metasomes in the production of HIMU-like magmatism on the northeast African
303 and Arabian plates: *Geology*, v. 42, p. 419–422, doi:10.1130/g35216.1.
- 304 Salters, V.J.M., and Stracke, A., 2004, Composition of the depleted mantle: *Geochemistry*,
305 *Geophysics, Geosystems*, v. 5, p. p.n/a, doi:10.1029/2003gc000597.

- 306 Sobolev, A.V. et al., 2007, The Amount of Recycled Crust in Sources of Mantle-Derived Melts:
307 Science, v. 316, p. 412–417, doi:10.1126/science.1138113.
- 308 Stracke, A., Hofmann, A.W., and Hart, S.R., 2005, FOZO, HIMU, and the rest of the mantle zoo:
309 Geochemistry, Geophysics, Geosystems, v. 6, p. Q05007- n/a, doi:10.1029/2004gc000824.
- 310 Stracke, A., Snow, J.E., Hellebrand, E., von der Handt, A., Bourdon, B., Birbaum, K., and Günther,
311 D., 2011, Abyssal peridotite Hf isotopes identify extreme mantle depletion: Earth and
312 planetary science letters, v. 308, p. 359–368, doi:10.1016/j.epsl.2011.06.012.
- 313 Tanaka, T., Togashi, S., Kamioka, H., Amakawa, H., Kagami, H., Hamamoto, T., Yuhara, M.,
314 Orihashi, Y., Yoneda, S., Shimizu, H., Kunimaru, T., Takahashi, K., Yunagi, T., Nakano, T.,
315 Fujimaki, H., Shinjo, R., Asahara, Y., Tanimizu, M., Dragusanu, C., 2000, JNdi-1: a
316 neodymium isotopic reference in consistency with LaJolla neodymium. Chemical Geology, v.
317 168, p. 279-281, doi:10.1016/S0009-2541(00)00198-4
- 318 Valdez-Moreno, G., Schaaf, P., Luis Macías, J., and Kusakabe, M., 2006, New Sr-Nd-Pb-O isotope
319 data for Colima volcano and evidence for the nature of the local basement, *in* Siebe, C., Luis
320 Macías, J., and Aguirre-Díaz, G.J. eds., Neogene-Quaternary Continental Margin Volcanism:
321 A perspective from México, Boulder, CO, Geological Society of America, v. 402, p. 45–63.
- 322 Waters, C.L., Sims, K.W.W., Perfit, M., Blichert-Toft, J., and Blusztajn, J., 2011, Perspective on the
323 Genesis of E-MORB from Chemical and Isotopic Heterogeneity at 9–10°N East Pacific Rise:
324 Journal of petrology, v. 52, p. 565–602, doi:10.1093/petrology/egq091.
- 325 Weiss, Y., Class, C., Goldstein, S., and Hanyu, T., 2016, Key new pieces of the HIMU puzzle from
326 olivines and diamond inclusions: Nature, v. 537, p. 666–670, doi:10.1038/nature19113.
- 327 Wittig, N., Pearson, D.G., Duggen, S., Baker, J., and Hoernle, K., 2010, Tracing the metasomatic and
328 magmatic evolution of continental mantle roots with Sr, Nd, Hf and and Pb isotopes: A case
329 study of Middle Atlas (Morocco) peridotite xenoliths: Geochimica et Cosmochimica Acta, v.
330 74, p. 1417–1435, doi:10.1016/j.gca.2009.10.048.
- 331 Woodhead, J.D., 1996, Extreme HIMU in an oceanic setting: the geochemistry of Mangaia Island
332 (Polynesia), and temporal evolution of the Cook—Austral hotspot: Journal of Volcanology
333 and Geothermal Research, v. 72, p. 1–19, doi:10.1016/0377-0273(96)00002-9.
- 334 Woodhead, J.D., Hergt, J.M., Giuliani, A., Phillips, D., and Maas, R., 2017, Tracking continental-scale
335 modification of Earth’s mantle using zircon megacrysts: International Kimberlite Conference
336 Extended Abstracts, vol. 11, nr. 11IKC-4575
- 337 Workman, R.K., and Hart, S.R., 2005, Major and trace element composition of the depleted MORB
338 mantle (DMM): Earth and planetary science letters, v. 231, p. 53–72,
339 doi:10.1016/j.epsl.2004.12.005.